Chemical Science

ROYAL SOCIETY OF CHEMISTRY

EDGE ARTICLE

View Article Online
View Journal | View Issue

Cite this: *Chem. Sci.*, 2022, **13**, 7566

All publication charges for this article have been paid for by the Royal Society of Chemistry

Received 5th May 2022
Accepted 3rd June 2022

DOI: 10.1039/d2sc02515a

rsc.li/chemical-science

Synthesis and hydrogenation of polycyclic aromatic hydrocarbon-substituted diborenes *via* uncatalysed hydrogenative B–C bond cleavage†

Alexander Okorn,[ab] Arumugam Jayaraman,[ab] Lukas Englert,[ab] Merle Arrowsmith,[ab] Theresa Swoboda,[ab] Jeanette Weigelt,[ab] Carina Brunecker,[ab] Merlin Hess,[ab] Anna Lamprecht,[ab] Carsten Lenczyk,[ab] Maximilian Rang[ab] and Holger Braunschweig *[ab]

The classical route to the PMe_3-stabilised polycyclic aromatic hydrocarbon (PAH)-substituted diborenes $B_2Ar_2(PMe_3)_2$ (Ar = 9-phenanthryl **7-Phen**; Ar = 1-pyrenyl **7-Pyr**) *via* the corresponding 1,2-diaryl-1,2-dimethoxydiborane(4) precursors, $B_2Ar_2(OMe)_2$, is marred by the systematic decomposition of the latter to $BAr(OMe)_2$ during reaction workup. Calculations suggest this results from the absence of a second *ortho*-substituent on the boron-bound aryl rings, which enables their free rotation and exposes the B–B bond to nucleophilic attack. **7-Phen** and **7-Pyr** are obtained by the reduction of the corresponding 1,2-diaryl-1,2-dichlorodiborane precursors, $B_2Ar_2Cl_2(PMe_3)_2$, obtained from the SMe_2 adducts, which are synthesised by direct NMe_2–Cl exchange at $B_2Ar_2(NMe_2)_2$ with $(Me_2S)BCl_3$. The low-lying π* molecular orbitals (MOs) located on the PAH substituents of **7-Phen** and **7-Pyr** intercalate between the B–B-based π and π* MOs, leading to a relatively small HOMO–LUMO gap of 3.20 and 2.72 eV, respectively. Under vacuum or at high temperature **7-Phen** and **7-Pyr** undergo intramolecular hydroarylation of the B=B bond to yield 1,2-dihydronaphtho[1,8-*cd*][1,2]diborole derivatives. Hydrogenation of **7-Phen**, **7-Pyr** and their 9-anthryl and mesityl analogues **III** and **II**, respectively, results in all cases in splitting of the B–B bond and isolation of the monoboranes $(Me_3P)BArH_2$. NMR-spectroscopic monitoring of the reactions, solid-state structures of isolated reaction intermediates and computational mechanistic analyses show that the hydrogenation of the three PAH-substituted diborenes proceeds *via* a different pathway to that of the dimesityldiborene. Rather than occurring exclusively at the B–B bond, hydrogenation of **7-Ar** and **III** proceeds *via* a hydroarylated intermediate, which undergoes one B–B bond-centered H_2 addition, followed by hydrogenation of the endocyclic B–C bond resulting from hydroarylation, making the latter effectively reversible.

Introduction

Since the isolation of the first neutral diborenes stabilised by two Lewis bases by Robinson and coworkers,[1,2] the synthesis of these very electron-rich boron-based alkene analogues and the exploration of their versatile reactivity has advanced greatly.[3,4] Symmetrical diborenes of the form $L_2B_2Y_2$ (where L is a neutral donor (*e.g.* N-heterocyclic carbene (NHC), cyclic alkyl(amino) carbene (CAAC), phosphine) and Y an anionic substituent (*e.g.* aryl, heteroaryl, alkyl, vinyl, halide, cyanide, hydride)) are most often synthesised either by the reductive coupling of two $LBYX_2$ precursors (X = halide),[3–10] or the reduction of 1,2-dihalodiboranes of the form $L_2B_2Y_2X_2$.[3,11–14] Since the apolar B–B bond of symmetrical diborenes often makes them relatively unreactive, recent efforts have also focused on synthesising polar, unsymmetrical diborenes by the reduction of unsymmetrically substituted 1,2-dihalodiboranes of the form $LL'B_2YY'X_2$.[15–20]

The stereoelectronic nature of the substituents of the B=B double bond greatly influences its reactivity by tuning the energies (and sometimes localisation) of the highest occupied and lowest unoccupied molecular orbitals (HOMO and LUMO). For example, changing the NHC and duryl ligands in diborene **I** (Fig. 1)[21] to PMe_3 and mesityl ligands, respectively, in **II**,[22] causes a decrease in the energy of the HOMO and an increase in the energy of the LUMO, thereby widening the HOMO–LUMO gap by *ca.* 0.7 eV.[23] In both **I** and **II**, the HOMO is localised on the B=B π bond, while the LUMO corresponds to the B–B π* orbital. When the mesityl substituents of **II** are changed to the polycyclic 9-anthryl (Anth) substituents of **III**,[12] the energy of the

[a]*Institute for Inorganic Chemistry, Julius-Maximilians-Universität Würzburg, Am Hubland, 97074 Würzburg, Germany. E-mail: h.braunschweig@uni-wuerzburg.de*

[b]*Institute for Sustainable Chemistry & Catalysis with Boron, Julius-Maximilians-Universität Würzburg, Am Hubland, 97074 Würzburg, Germany*

† Electronic supplementary information (ESI) available: Synthetic procedures, NMR, HRMS and UV-vis data, X-ray crystallographic and computational details. CCDC 2169207–2169215. For ESI and crystallographic data in CIF or other electronic format see **https://doi.org/10.1039/d2sc02515a**

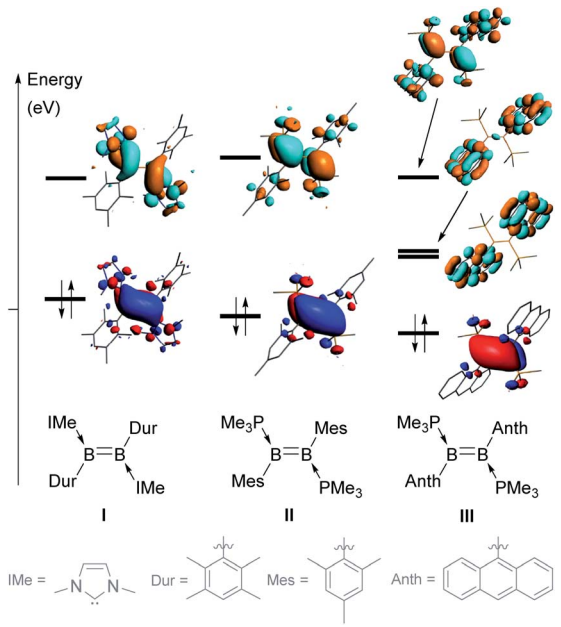

Fig. 1 Comparison of the frontier molecular orbitals (MOs) of diborenes I, II and III.

HOMO is slightly lowered but, most importantly, two of the π* orbitals of the anthryl fragments (in-phase and anti-phase) intercalate between the B–B π and π* orbitals (usually the frontier orbitals), thereby lowering the HOMO–LUMO gap to only 1.07 eV. This orbital intercalation adds to the usual B–B bond-centred reactivity of diborenes the possibility of aryl-centred reactivity, as borne out by the intramolecular C–H borylation of the anthryl moiety in reactions with selenium and copper triflate.[12,24]

Thus far, all known diaryldiborenes bear very sterically demanding aryl substituents, substituted in both *ortho* positions, which locks these substituents in a position orthogonal to the plane of the diborene core. In order to increase the reactivity of diaryldiborenes even further we aimed to synthesise new polycyclic aromatic hydrocarbon (PAH)-substituted diborenes with a similar frontier orbital arrangement as **III**, but in which the boron-bound aryl ring bears only one *ortho* substituent, such as the 9-phenanthryl and 1-pyrenyl groups displayed in Scheme 1. In this study, we show that the unsymmetrical nature and diminished steric profiles of the 9-phenanthryl and 1-pyrenyl substituents first of all necessitate a different synthetic route to the desired PMe_3-stabilised diphenanthryl- and dipyrenyldiborenes, and secondly make the latter thermally unstable towards intramolecular C–H borylation. Furthermore, we examine the hydrogenation mechanism of PAH-substituted diborenes relative to that of the dimesityldiborene **III**, both experimentally and computationally.

Results and discussion

Synthesis of PAH-substituted diborane precursors

Literature-known phosphine-stabilised 1,2-diaryldiborenes such as **II** and **III** are synthesized by twofold reduction of the 1,2-diaryl-1,2-dibromodiborane precursors, $B_2Ar_2Br_2$ (**3-Ar**), in the presence of PMe_3.[12,22] The precursors **3-Ar** are obtained *via* a three-step procedure by (a) arylation of $B_2X_2(NMe_2)_2$ (X = Cl, Br) with LiAr to yield **1-Ar**, followed by (b) acidic methanol quenching to yield **2-Ar**, and finally (c) bromination to yield **3-Ar** (Scheme 1).[25–27] Attempts to synthesise the corresponding diphenanthryl- and dipyrenyldiboranes(4) following the same procedure failed as step (b) was systematically followed by B–B bond cleavage of **2-Ar** during workup. Although **2-Ar** was detected in the ^{11}B NMR spectrum of the reaction mixture at *ca.* 59 ppm (**2-Mes**: δ_{11B} = 61 ppm),[26] workup systematically led to the isolation of the dimethoxyboranes **4-Ar** (δ_{11B} = *ca.* 31 ppm, *cf.* **4-Ph**: δ_{11B} = 28.1 ppm)[28] as the sole isolable products (Scheme 1d). Multiple attempts to isolate **2-Ar** using different stoichiometries (2.1 equiv. MeOH and HCl), HCl solutions (in Et_2O or toluene), solvents (Et_2O, toluene, benzene, hexane), workup temperatures (0 °C, rt) and procedures (extraction, precipitation, neutralisation of ammonium salt by-product) all led to the isolation of the monoboranes **4-Ar** as the major product in up to 77% yield (see ESI† for details).

Since **2-Mes** and **2-Anth**, in which the boron-bound aryl rings are substituted in both *ortho* positions, are stable, the origin of the instability of **2-Phen** and **2-Pyr** must lie in the absence of a second *ortho* substituent. This results in a lower barrier to rotation of the aryl substituents. Calculations at the M06/6-31g(d,p) level of theory show that **2-Phen** and **2-Pyr** each have three stable rotational isomers, depending on the relative orientation of the two unsymmetrical aryl substituents (Fig. 2). For the pyrenyl derivative the most stable isomer is **2a-Pyr**, in which the *ortho* protons point in opposite directions, maximizing π overlap between the parallel polycyclic aromatic groups by minimising the (C–B–B–C) torsion angle (**2a-Pyr** 22.2°). For comparison, the (C–B–B–C) torsion angles in the solid-state structures of **2-Mes** and **2-Anth** are *ca.* 104° and 125°, respectively.[12,26] The isomer in which both *ortho* protons point towards each other, **2b-Pyr**, is of similar energy to **2a-Pyr**. The third isomer, in which both *ortho* protons point in the same direction, **2c-Pyr**, lies only 2.0 kcal mol^{-1} higher in energy than

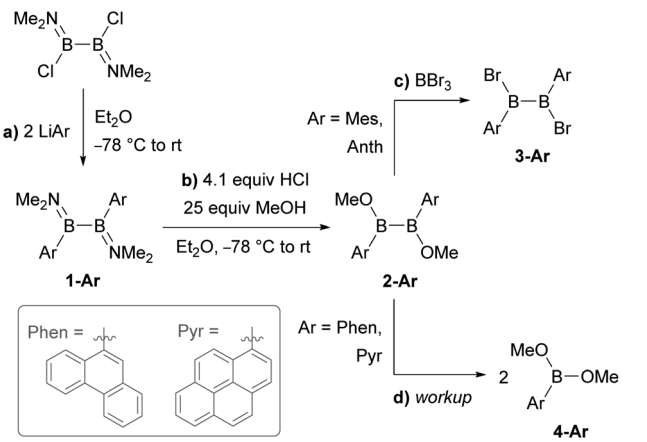

Scheme 1 Attempted synthesis of $B_2Ar_2Br_2$ (**3-Ar**, Ar = Phen, Pyr) *via* $B_2Ar_2(OMe)_2$ (**2-Ar**).

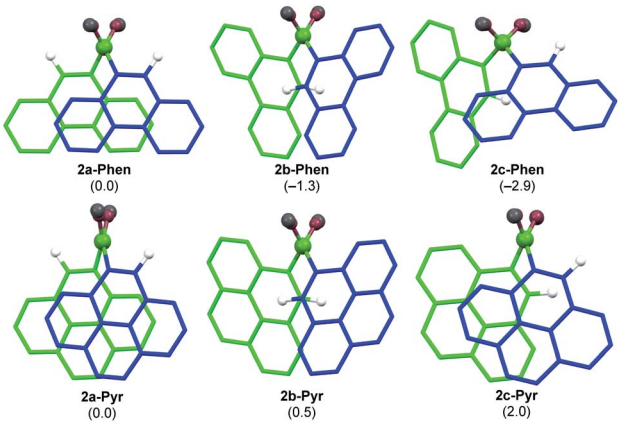

Fig. 2 Calculated rotational isomers of **2-Phen** and **2-Pyr** optimised at the M06/6-31g(d,p) level of theory, viewed along the B–B axis. Hydrogen atoms omitted for clarity, except for the *ortho* protons. Blue framework: front aryl group; green framework: back aryl group. Atom colours: white, H; fir green, B; dark red, O; dark grey, C. Relative free energies in parentheses in kcal mol^{-1}.

2a-Pyr. For the phenanthryl derivative the trend is reversed, **2c-Phen** being 2.9 kcal mol^{-1} more stable than **2a-Phen**, in which the π overlap is far less pronounced than in **2a-Pyr**, due to a much larger (C–B–B–C) torsion angle of 65°. In both cases, however, the asymmetry of the energetically accessible **2c-Ar** conformation, combined with the much lower steric protection afforded by the 9-phenanthryl and 1-pyrenyl ligands when compared to the mesityl and 9-anthryl ligands, may be the cause of the increased instability of **2-Phen** and **2-Pyr**, presumably promoting nucleophilic attack of unreacted MeOH at the B–B bond. The exact mechanism of the conversion from the diboranes **2-Ar** to the monoboranes **4-Ar**, however, remains unclear.

An alternative route was envisaged by direct NMe_2–Br exchange using $(Me_2S)BBr_3$ as the bromide source.[29] While **1-Ar** (Ar = Phen, Pyr) underwent NMe_2–Br exchange with $(Me_2S)BBr_3$ as shown by the formation of $BBr_2(NMe_2)$ (δ_{11B} = 26 ppm),[30] the reaction did not yield the desired 1,2-diaryl-1,2-dibromodiborane, but instead a complex mixture of products, including some resulting from B–B bond splitting. In contrast, the reaction of **1-Ar** (Ar = Phen, Pyr) with 2.1 equiv. $(Me_2S)BCl_3$ in benzene proceeded cleanly over a period of 5 days at room temperature to afford the SMe_2-stabilised precursors **5-Ar** in 90% (Ar = Phen) and 84% (Ar = Pyr) isolated yields (Scheme 2a). The addition of 2 equiv. PMe_3 to **5-Ar** resulted in quantitative conversion to the doubly PMe_3-stabilised 1,2-diaryl-1,2-dichlorodiboranes, **6-Ar** (δ_{11B} = 1.3 ppm), isolated in 83% (Ar = Phen) and 86% (Ar = Pyr) yields (Scheme 2b).

The solid-state structures of **6-Phen** and **6-Pyr** show an unexpected eclipsed conformation of the substituents at the two boron atoms (C–B–B–C and P–B–B–Cl torsion angles 10.1–14.8°, Fig. 3). This contrasts with the staggered conformation usually observed in doubly base-stabilized di- and tetrahalodiboranes, which minimises steric repulsion.[31–34] The eclipsed conformation might be favoured in this case by attractive interactions between the two PAH groups. The B–B bond lengths of 1.776(4) and 1.779(7) Å for **6-Phen** and **6-Pyr**, respectively, are within the range typical for acyclic doubly base-stabilised diboranes.[31–34]

Synthesis of PAH-substituted diborenes

The reduction of **6-Ar** with 2.5 equiv. KC_8 in a 5 : 1 benzene–THF solvent mixture at room temperature over a period of 4 h resulted in a colour change to red for **7-Phen** and blue for **7-Pyr** (Scheme 2c). NMR spectra of the filtered reaction mixtures showed 60–80% conversion to the diborenes **7-Ar**, which display a broad ^{11}B NMR resonance at *ca.* 21 ppm and a broad ^{31}P NMR singlet at *ca.* −22 ppm, similar to the dianthryldiborene **III** (δ_{11B} = 22 ppm, δ_{31P} = −21.3 ppm).[12] Interestingly, the ^{1}H NMR spectrum of **7-Phen** showed the presence of two isomers, which were identified as two rotamers of **7-Phen**, the centrosymmetric species **7a-Phen** and its isomer **7b-Phen**, in which one of the phenanthryl substituents is rotated by 180° compared to **7a-Phen** (Fig. 5). Calculations showed that these two rotamers are only 0.4 kcal mol^{-1} apart in energy (see ESI† for details), which is in agreement with their experimentally observed formation in a nearly 1 : 1 ratio. The UV-vis spectrum of **7-Phen** showed several strong, overlapping absorptions in the 350–400 nm

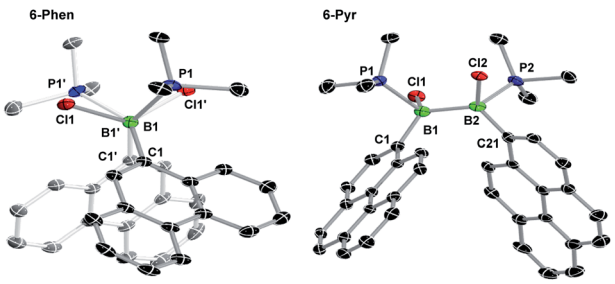

Fig. 3 Crystallographically-derived solid-state structures of **6-Phen** (view along the B–B axis showing the eclipsed conformation) and **6-Pyr**. Atomic displacement ellipsoids at 50%. Hydrogen atoms omitted for clarity. Selected bond lengths (Å) and angles (°) for **6-Phen**: B1–B1′ 1.776(4), B1–P1 1.9950(19), B1–Cl1 1.9719(19), B1–C1 1.629(2), torsion C1–B1–B1′–C1′ 14.4(2); for **6-Pyr**: B1–B2 1.779(7), B1–P1 1.997(5), B1–Cl1 1.974(5), B1–C1 1.637(7), B2–P2 2.005(5), B2–Cl2 1.969(5), B1–C21 1.634(6), torsion C1–B1–B2–C21 13.3(6).

Scheme 2 Synthetic route to the diborenes $B_2Ar_2(PMe_3)_2$ (**7-Ar**) *via* the diaryl(dichloro)diborane precursors **5-Ar** and **6-Ar**.

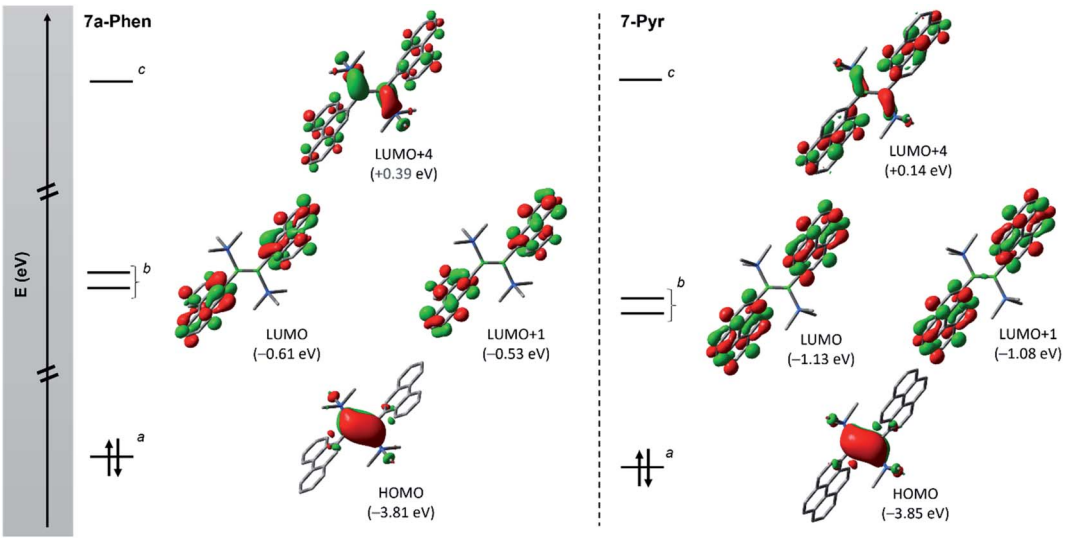

Fig. 4 Frontier orbitals (isovalue: ±0.04) of diborenes **7a-Phen** (left) and **7-Pyr** (right) showing the orbital intercalation between PAH and diborene units. [a] π orbital of the B=B bond; [b] π* orbitals of PAH units; and [c] π* orbital of the B=B bond. Note: molecular orbitals LUMO+2 and LUMO+3 corresponding to other combination of π* orbitals of PAH units are not shown (see ESI†).

range and a low-intensity broad absorption band centred around 480 nm, accounting for its red colour. Unfortunately, **7-Pyr** was too unstable in solution to acquire meaningful UV-vis data.

A single-crystal X-ray diffraction analysis of **7a-Phen** confirmed the formation of the diborene (Fig. 5). The structure was entirely disordered in a 1 : 1 ratio *via* a mirror plane orthogonal to the plane of the B=B unit and bisecting the B–B bond, thus precluding a detailed analysis of bonding parameters (see ESI† for details). The same disorder was also found in the solid-state structure of the anthryl analogue **III**.[12] The B–B bond length of *ca.* 1.56 Å (average of the two overlapping diborenes) is within the range usually observed in diborenes (1.52–1.62 Å).[1,12,21,35]

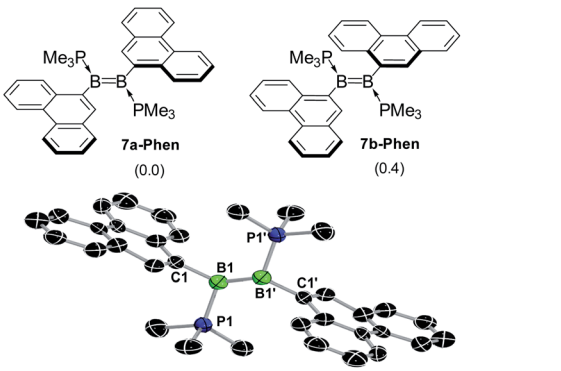

Fig. 5 Top: the two rotamers of **7-Phen**, **7a-Phen** and **7b-Phen**. Energies (kcal mol^{-1}) in parentheses calculated at the M06/6-31g(d,p)/SMD(THF) level of theory. Bottom: crystallographically-derived solid-state structure of **7a-Phen**. Atomic displacement ellipsoids at 50%. Ellipsoids of ligand periphery and hydrogen atoms omitted for clarity. Structural parameters cannot be discussed due to heavy structural disorder and bonding restraints applied during refinement.

The computed structure of **7a-Phen** also displays a very similar B–B bond length (1.57 Å, see ESI†). Additionally, the π core of the B=B double bond and that of the phenanthryl units are likely unconjugated, as the C2–C1–B1–B1′ torsion angle is *ca.* 78.7°. The computed structure of **7-Pyr** also shows a very similar B–B bond length (1.575 Å) and a larger C2–C1–B1–B1′ twist of 105.4°.

Fig. 4 depicts the frontier molecular orbitals (MOs) of **7a-Phen** and **7-Pyr**. For comparison, such details were also computed for diborene **III** at the same level of theory (see ESI†). Diborenes **7a-Phen** and **7-Pyr** exhibit a similar arrangement of frontier orbitals and orbital energies as **III**, with the low-lying unoccupied π* orbitals of the phenanthryl and pyrenyl residues intercalated between the π and π* orbitals of the B–B bond to furnish a small HOMO–LUMO gap (HLG). As in **III**,[12] the HOMO of **7a-Phen** and **7-Pyr** is a B–B π-bonding orbital, and the LUMO and LUMO+1 are in-phase and anti-phase π* orbitals, respectively, exclusively spread over both PAH units. Energetically, the frontier MOs HOMO to LUMO+4 in all three diborenes lie in a similar range (−3.85 eV to +0.39 eV). In terms of engineering a small HLG in diborenes by incorporating PAH substituents, phenanthryl and pyrenyl groups show no advantage over anthryl groups, even if the HLG of **7-Pyr** is close to that of **III** (HLGs for **7a-Phen**: 3.20 eV; **7-Pyr**: 2.72 eV; **III**: 2.53 eV).[12]

During the reduction of **6-Ar** to **7-Ar**, a small amount of by-product **8-Ar** was formed, which displays two broad ^{11}B NMR resonances at −13 and −22 ppm, and two broad ^{31}P NMR doublets at −5 and −9 ppm ($^{3}J_{PP}$ = 84 Hz), indicative of an unsymmetrical doubly PMe_3-stabilised diborane. Upon removing all volatiles *in vacuo*, the diborene **7-Ar** converted entirely to **8-Ar**, isolated as a colourless solid in 50% yield for Ar = Phen and as a yellow solid in 55% yield for Ar = Pyr (Scheme 3). The ^{1}H NMR spectrum of **8-Phen** showed a very broad B*H* resonance in the 2.4–3.2 ppm region, which resolved to an apparent triplet upon ^{11}B decoupling ($^{2/3}J_{HP}$ = 17.0 Hz).

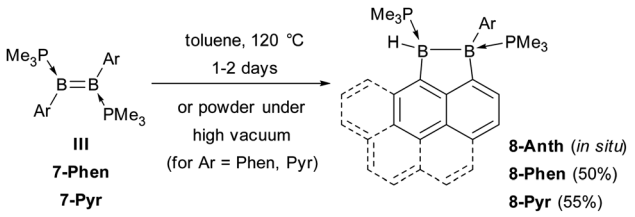

Scheme 3 Intramolecular C–H activation in diborenes III and 7-Ar.

A single-crystal X-ray analysis showed that **8-Phen** is the product of the intramolecular hydroarylation of diborene **7-Phen**, which generates a doubly PMe_3-stabilised 4-(9-phenanthryl)-5-hydro-phenanthro[1,10-*cd*][1,2]diborole (Fig. 6). A similar intramolecular hydroarylation reaction has been observed for **III**, triggered by the coordination of copper triflate to the B=B double bond and followed by hydride abstraction and PMe_3 migration,[36] as well as for a 9-anthryl-substituted disilane under photolytic conditions.[37] In the case of **7-Phen** and **7-Pyr** this reaction can be triggered either by removal of all volatiles from the reaction mixture (free PMe_3 in the reaction mixture seems to stabilise **7-Ar**) or by heating the reaction mixture for 2 days at 120 °C for complete conversion. The anthryl derivative **III** could also be partially converted to **8-Anth** over a period of several days in refluxing toluene but was stable under vacuum. This increased reactivity of **7-Phen** and **7-Pyr** compared to **III** is likely due to the lower steric shielding of the boron centres provided by the unsubstituted *ortho* position of the 9-phenanthryl and 1-pyrenyl ligands. The B–B bond in **8-Phen** (1.795(2) Å) is slightly longer than in the hydroarylated anthryl derivative (1.782(2) Å)[36] due to the additional presence of the hydride ligand at B1. The phenanthro[1,10-*cd*][1,2]diborole ring is not fully planar and shows a slight curvature of the PAH backbone (the mean planes of the three C_6 rings form angles of 1.9 and 4.1° between each other) and a slight twist in the 1,2-diborole ring (torsion angles C1–B1–B2–C3 11.35(11), C2–C3–B2–B1 −9.43(12), C2–C1–B1–B2 −10.70(12)°) caused by the ring strain of the C_3B_2 ring.

Hydrogenation of $B_2Ar_2(PMe_3)_2$

Heating a toluene solution of **III** or **7-Ar** at 120 °C for 5 days under 1 bar of H_2 resulted in twofold hydrogenation and

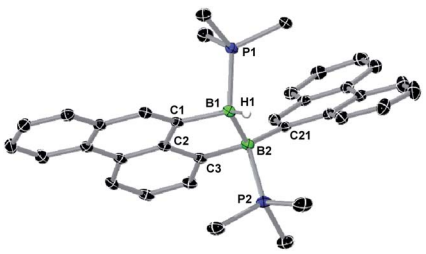

Fig. 6 Crystallographically-derived solid-state structure of **8-Phen**. Atomic displacement ellipsoids at 50%. Hydrogen atoms omitted for clarity, except boron-bound H1.‡ Selected bond lengths (Å) and angles (°): B1–B2 1.795(2), B1–P1 1.9348(17), B1–C1 1.6221(18), B1–H1 1.148(17), B2–P2 1.9806(17), B2–C21 1.6230(19), B2–C3 1.6381(18).

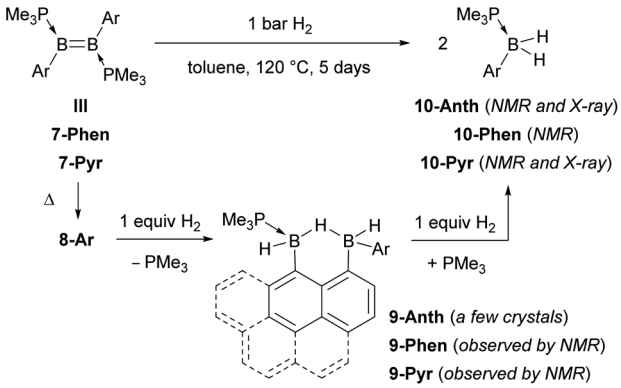

Scheme 4 Hydrogenation of III and 7-Ar.

splitting of the B–B bond to yield the phosphine-stabilised arylboranes **10-Ar**, characterised by an $^{11}B\{^1H\}$ NMR doublet at *ca.* −25 ppm ($^2J_{BP} \approx 50$ Hz) and a broad $^{31}P\{^1H\}$ NMR multiplet around −8 ppm (Scheme 4). During the course of these reactions an intermediate, **9-Ar**, with two ^{11}B NMR resonances in a 1 : 1 ratio at around −23 and −27 ppm, was observed but could not be isolated. The hydrogenation of the known diborene **III** in toluene at 120 °C under 1 bar of H_2, however, proceeded more slowly, leading to the isolation of a few crystals of the intermediate **9-Anth** suitable for X-ray diffraction analysis after 2 days. The solid-state structure of **9-Anth** shows a hydride-bridged 9-boranylanthracene-1-yl(anthrylborane), stabilised by a single PMe_3 ligand, which results from the single hydrogenation of the B–B bond of **8-Anth** with loss of one PMe_3 ligand (Fig. 7). In the reaction shown in Scheme 4, this first step is followed by the addition of a second equivalent of H_2 across the B2–C3 bond of **9-Ar**, yielding **10-Ar** and $ArBH_2$, the latter forming an adduct with the remaining PMe_3 ligand to yield the second equivalent of **10-Ar**.

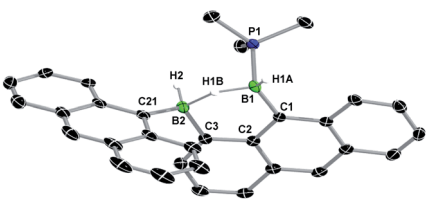

Fig. 7 Crystallographically-derived solid-state structure of **9-Anth**. Atomic displacement ellipsoids at 50%. Hydrogen atoms omitted for clarity, except boron-bound hydrides.‡ Selected bond lengths (Å) and angles (°): B1–P1 1.948(3), B1–C1 1.597(4), B1–H1A 1.11(4), B1–H1B 1.26(4), B2–H1B 1.41(4), B2–H2 1.12(3), B2–C21 1.611(13), B2–C3 1.600(4).

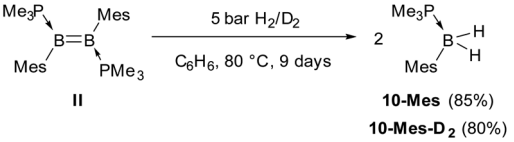

Scheme 5 Hydrogenation of II.

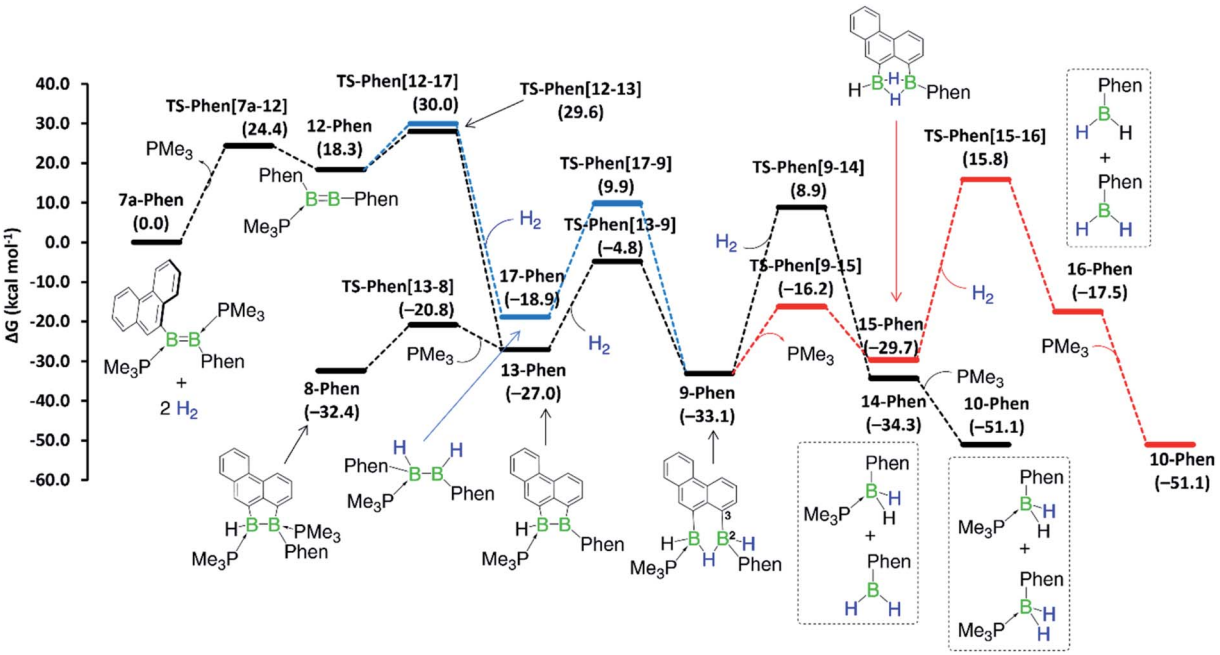

Fig. 8 Mechanisms computed for the hydrogenation of diborene **7-Phen** at the M06/6-31g(d,p)/SMD(toluene) level of theory. Black profile: hydrogenation *via* initial H–H activation pathway; blue profile: hydrogenation *via* initial C–H activation pathway; and red profile: second hydrogenation entailing the bis(monoborane) intermediate **15-Phen**. Free energies in parentheses.

The reaction is remarkable in that it involves the uncatalysed hydrogenative cleavage of a strong B–C bond, thus effectively rendering the intramolecular hydroarylation process reversible. To our knowledge, the only other example of B–C bond-cleaving hydrogenation is the palladium-catalysed hydrogenation of a boratirene, resulting in ring-opening of the strained BC_2 heterocycle.[38] Interestingly, Piers proposed that the formation of *cis*- and *trans*-isomers in the 2,5-hydrogenation of pentaarylboroles can be explained by the first reaction step being the 1,2-hydrogenation of the endocyclic B–C bond, followed by rotation of the remaining B–C bond and finally cyclisation to the *cis*/*trans*-boracyclopent-3-ene. The putative ring-opened 1,3-butadienylborane intermediate of this reversible B–C bond-cleaving hydrogenation, however, was not detected.[39]

In comparison, the hydrogenation of the related dimesityldiborene **II** required heating in benzene for 9 days at 80 °C under 5 bar of H_2 (Scheme 5). Although the final product of the hydrogenation was also the phosphine-stabilised arylborane **10-Mes**, NMR-spectroscopic monitoring during the course of the reaction did not show any intermediates. In contrast, the hydrogenation of the related diiododiborene $B_2I_2(PMe_3)_2$ proceeded stepwise, enabling the isolation of the single hydrogenation intermediate $B_2I_2H_2(PMe_3)_2$.[40]

Mechanistic computational analyses

Although a similar hydrogenation mechanism to that of **III**, **7-Phen** and **7-Pyr** may be envisaged for diborene **II**, since mesityl-substituted diboron compounds are known to undergo intramolecular C–H activation at one *ortho*-methyl group to form a 2-benzyl unit bridging two boron centres,[41,42] the known hydrogenation mechanism for $B_2I_2(PMe_3)_2$ *via* $B_2I_2H_2(PMe_3)_2$[40] makes a similar stepwise hydrogenation of **II** *via* $B_2Mes_2H_2(PMe_3)_2$ more likely. We envisage that the initial competition for activating the intramolecular aryl C–H bond of fused arenes or the H–H bond of H_2 by the diborenes, after PMe_3 dissociation, decides the fate of the mechanism. This view puts forward that diborenes **7-Phen**, **7-Pyr** and **III** perhaps follow the C–H activation route, while diborene **II**, lacking a nearby aryl C–H bond, may follow the H–H activation route. To ascertain this, computations were performed on both pathways for all diborenes. The pathways computed for **7a-Phen** and **II** are shown in Fig. 8 and 9, respectively. Since diborenes **7-Pyr** and **III** pose similar mechanistic steps and energetics to **7a-Phen**, their free energy profiles are provided in the ESI (Fig. S80 and S81,† respectively). The most likely reaction pathway with the lowest barriers is provided as a black profile.

The twofold hydrogenation of all diborenes to the boranes **10-Ar** is substantially exergonic, with ΔG ranging from −47.6 to −51.1 kcal mol^{-1}. Although the initial step of PMe_3 dissociation from all diborenes, leading to intermediate **12-Ar**, is significantly endergonic, it has a relatively low energy barrier of 22.7 to 24.4 kcal mol^{-1}. In the next step, intermediates **12-Phen**, **12-Pyr** and **12-Anth** all show almost an equal propensity towards C–H (black profile) and H–H activation (blue profile), with the overall energy barriers for these two processes from **7-Ar** and **III** separated by only 0.4 to 2.1 kcal mol^{-1} (Fig. 8, S80 and S81†). For these PAH-substituted diborenes the formation of both **13-Ar** and **17-Ar**, and eventually both mechanisms, are therefore energetically accessible. Nevertheless, the experimentally observed intermediate **8-Ar**, formed by reassociation of PMe_3 to **13-Ar**, is in all cases thermodynamically favoured over the direct

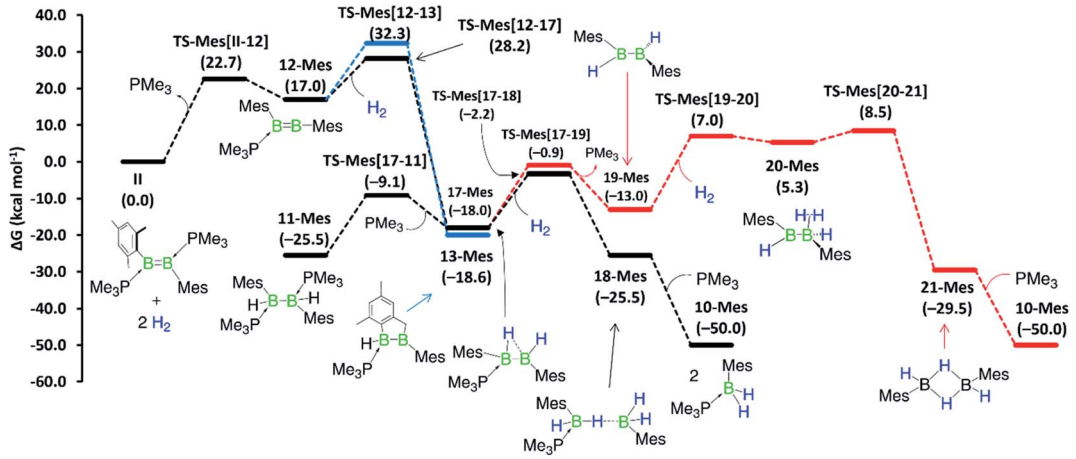

Fig. 9 Mechanisms computed for the hydrogenation of diborene II at the M06/6-31g(d,p)/SMD(benzene) level of theory. Black profile: hydrogenation *via* initial H–H activation pathway and the more likely pathway; blue profile: hydrogenation *via* initial C–H activation pathway; and red profile: second hydrogenation involving the diborane(4) intermediate **19-Mes**. Free energies in parentheses.

hydrogenation intermediate **17-Ar** by 5.5 to 13.5 kcal mol^{-1}. Both pathways lead to intermediate **9-Ar**, in one case by C–H activation of one aryl moiety at **17-Ar**, in the other by hydrogenation of **13-Ar**. As mentioned above, **9-Ar** forms the product **10-Ar** by consuming the second equivalent of H_2 *via* direct H–H activation across the B2–C3 bond in **9-Ar**, followed by PMe_3 association. If we consider **9-Ar** as the major resting species, the activation of the second H_2 equivalent by **9-Ar**, leading to **14-Ar**, *i.e.* the hydrogenative cleavage of the endocyclic B–C bond, becomes rate-limiting ($\Delta G^{\ddagger} \approx 42$ kcal mol^{-1}, **TS-Ar(9–14)**) and explains the high reaction temperature required for full conversion. The alternative pathway, *via* loss of PMe_3 to generate **15-Ar**, followed by H_2 activation (red profile), is energetically less favourable by 3 to 5 kcal mol^{-1}.

Competition for the initial C–H or H–H activation is not seen with diborene **II**, as activating the *ortho*-methyl C–H bond of the mesityl substituent is energetically less favoured ($\Delta G^{\ddagger} = 32.3$ kcal mol^{-1}, **TS-Mes(12–13)**) than the activation of H_2 ($\Delta G^{\ddagger} = 28.2$ kcal mol^{-1}, **TS-Mes(12–17)**, Fig. 9). Thus, intermediate **12-Mes** undergoes H_2 activation across the B=B bond, leading to the resting species, the doubly PMe_3-stabilised 1,2-dihydro-1,2-dimesityldiborane **11-Mes**. This species loses one PMe_3, leading to the hydride-bridged diborane **17-Mes**, which activates the second equivalent of H_2 across the B–B single bond, ultimately forming the product **10-Mes**. Following previous reports of symmetrical di- and tetraaryldiboranes(4) spontaneously activating dihydrogen across their B–B bond,[43,44] this pathway was also computed using the diborane(4) intermediate **19-Mes**, generated from **17-Mes** through PMe_3 dissociation, but proved less competitive for the formation of **10-Mes** (red profile). For the whole hydrogenation reaction of diborene **II**, the first H_2 activation step (**II**-to-**17-Mes**) is rate-limiting ($\Delta G^{\ddagger} = 28.2$ kcal mol^{-1}).

Overall, computations reveal that for diborenes **7-Phen**, **7-Pyr** and **III**, both C–H and H–H activation pathways initially compete almost equally to establish the observed resting species **9-Ar**, while the second H_2 addition proceeds directly across the B–C bond of **9-Ar**. In contrast, for diborene **II**, it is clear-cut that both the first and second hydrogenation occur essentially across the B–B core.

Conclusions

Unlike the straightforward syntheses of the PMe_3-stabilised dimesityl- and dianthryldiborenes **II** and **III**, the synthesis of the analogous 9-phenanthryl and 1-pyrenyl-substituted diborenes **7-Phen** and **7-Pyr** is fraught with complications owed to the absence of a second *ortho* substituent at the boron-bound aryl rings. The reduced steric bulk of these PAH substituents enables their free rotation, thus exposing the B–B bond of both diborane precursors and diborenes to decomposition. Systematic B–B bond cleavage during the usual synthetic route *via* $B_2Ar_2(OMe)_2$ precursors can be circumvented by direct NMe_2–Cl exchange at $B_2Ar_2(NMe_2)_2$ precursors with $(Me_2S)BCl_3$. The resulting isolable SMe_2 adducts of $B_2Ar_2Cl_2$ can be converted to the PMe_3 adducts, which can in turn be reduced to the desired diborenes **7-Phen** and **7-Pyr**. The facile rotation of the 9-phenanthryl substituent is evidenced by the existence of two energetically equivalent rotational isomers of **7-Phen** in solution. DFT calculations show that, as in **III**, the low-lying unoccupied π* orbitals of the PAH residues of **7-Phen** and **7-Pyr** are intercalated between the π and π* orbitals of the B–B bond to furnish a small HOMO–LUMO gap, albeit a slightly larger one than in **III**. Both **7-Phen** and **7-Pyr** were only stable in solution at rt in the presence of PMe_3, thus marring their clean isolation in the solid state. At high temperature in solution or under vacuum **7-Phen** and **7-Pyr** underwent intramolecular hydroarylation of the B=B bond to yield the 1,2-dihydronaphtho[1,8-*cd*][1,2]diborole derivatives **8-Ar**. The analogous **8-Anth** could also be obtained, albeit in much lower yield, by refluxing **III** in toluene for several days.

The twofold hydrogenation of the PAH-substituted diborenes with 1 bar H_2 required prolonged reaction times and high temperatures. NMR-spectroscopic monitoring of the reactions

showed that they proceeded through the formation of the hydroarylation intermediates **8-Ar**, followed by hydrogenation of one boron moiety of **8-Ar** to yield the intermediates **9-Ar**, of which the anthryl derivative was structurally characterised, and finally a second hydrogenation of the B–C bond resulting from hydroarylation to yield the monoboranes $(Me_3P)BArH_2$ (**10-Ar**). The hydrogenation of the mesityl derivative **II**, which required 5 bar H_2, longer reactions times and yielded the analogous monoborane **10-Mes**, did not show any stable reaction intermediates. Computational mechanistic analyses using DFT showed that the hydrogenation of **II** proceeds by two successive H_2 additions to the B–B bond. In contrast, hydrogenation of the PAH derivatives can proceed either *via* H_2 addition at the B–B bond first and intramolecular hydroarylation second, or *vice versa*, both pathways converging in the second H_2 addition, which splits the B–C bond formed in the hydroarylation step. This unprecedented, uncatalysed hydrogenative B–C bond cleavage constitutes the rate-limiting step and effectively reverses the intramolecular hydroarylation process.

Finally, it must be noted that the use of phenanthryl and pyrenyl substituents in both diborane and diborene chemistry affords clear disadvantages over hitherto employed aryl substituents. This is due on the one hand to the lack of steric protection of the B–B bond, which often leads to decomposition, on the other hand to the insoluble nature of both the desired products and side products, which frustrates efforts to purify the compounds.

Data availability

The datasets supporting this article have been uploaded as part of the ESI.†

Author contributions

A. O. designed and carried out 90% of the experimental work. L. E., T. S. and J. W. carried out the remaining 10% of the experimental work. A. J. carried out the majority of theoretical calculations. M. A. wrote the manuscript, refined X-ray structures and carried out preliminary computations. A. O., A. J., L. E. and M. A. co-wrote the ESI. C. B., M. H., A. L., C. L. and M. R. carried out X-ray crystallographic experiments. H. B. designed the original project and provided the funding.

Conflicts of interest

There are no conflicts to declare.

Acknowledgements

This project was funded by the European Research Council (ERC) under the European Union Horizon 2020 Research and Innovation Program (grant agreement no. 669054). A. J. thanks the Alexander von Humboldt Foundation (Germany) and NSERC (Canada) for postdoctoral fellowships.

Notes and references

‡ The boron-bound hydrides were detected in the inverse Fourier map and freely refined.

1 Y. Wang, B. Quillian, P. Wei, C. S. Wannere, Y. Xie, R. B. King, H. F. Schaefer III, P. v. R. Schleyer and G. H. Robinson, *J. Am. Chem. Soc.*, 2007, **129**, 12412.
2 Y. Wang, B. Quillian, P. Wei, Y. Xie, C. S. Wannere, R. B. King, H. F. Schaefer III, P. v. R. Schleyer and G. H. Robinson, *J. Am. Chem. Soc.*, 2008, **130**, 3298.
3 M. Arrowsmith, H. Braunschweig and T. E. Stennett, *Angew. Chem., Int. Ed.*, 2017, **56**, 96.
4 C. Weetman, *Chem.–Eur. J.*, 2021, **27**, 1941.
5 A. Hermann, M. Arrowsmith, D. E. Trujillo-Gonzalez, J. O. C. Jiménez-Halla, A. Vargas and H. Braunschweig, *J. Am. Chem. Soc.*, 2020, **142**, 5562.
6 U. Schmidt, F. Fantuzzi, M. Arrowmsith, A. Hermann, D. Prieschl, A. Rempel, B. Engels and H. Braunschweig, *Chem. Commun.*, 2020, **56**, 14809.
7 D. Auerhammer, M. Arrowsmith, P. Bissinger, H. Braunschweig, T. Dellermann, T. Kupfer, C. Lenczyk, D. K. Roy, M. Schäfer and C. Schneider, *Chem.–Eur. J.*, 2018, **24**, 266.
8 A. Hermann, F. Fantuzzi, M. Arrowsmith, T. Zorn, I. Krummenacher, B. Ritschel, K. Radacki, B. Engels and H. Braunschweig, *Angew. Chem., Int. Ed.*, 2020, **59**, 15717.
9 H. Braunschweig, I. Krummenacher, C. Lichtenberg, J. D. Mattock, M. Schäfer, U. Schmidt, C. Schneider, T. Steffenhagen, S. Ullrich and A. Vargas, *Angew. Chem., Int. Ed.*, 2017, **56**, 889.
10 A. Hermann, J. Cid, J. D. Mattock, R. D. Dewhurst, I. Krummenacher, A. Vargas, M. J. Ingleson and H. Braunschweig, *Angew. Chem., Int. Ed.*, 2018, **57**, 10091.
11 J. H. Müssig, M. Thaler, R. D. Dewhurst, V. Paprocki, J. Seufert, J. D. Mattock, A. Vargas and H. Braunschweig, *Angew. Chem., Int. Ed.*, 2019, **58**, 4405.
12 S. R. Wang, M. Arrowsmith, J. Böhnke, H. Braunschweig, T. Dellermann, R. D. Dewhurst, H. Kelch, I. Krummenacher, J. D. Mattock, J. H. Müssig, T. Thiess, A. Vargas and J. Zhang, *Angew. Chem., Int. Ed.*, 2017, **56**, 8009.
13 A. Stoy, M. Arrowsmith, M. Eyßelein, T. Dellermann, J. Mies, K. Radacki, T. Kupfer and H. Braunschweig, *Inorg. Chem.*, 2021, **60**, 12625.
14 J. Fan, M.-C. Yang, M.-D. Su and C.-W. So, *Inorg. Chem.*, 2021, **60**, 16065.
15 J. Fan, J.-Q. Mah, M.-C. Yang, M.-D. Su and C.-W. So, *J. Am. Chem. Soc.*, 2021, **143**, 4993.
16 W. Lu, A. Jayaraman, F. Fantuzzi, R. D. Dewhurst, M. Härterich, M. Dietz, S. Hagspiel, I. Krummenacher, K. Hammond, J. Cui and H. Braunschweig, *Angew. Chem., Int. Ed.*, 2022, **61**, e202113947.
17 T. E. Stennett, J. D. Mattock, I. Vollert, A. Vargas and H. Braunschweig, *Angew. Chem., Int. Ed.*, 2018, **57**, 4098.
18 W. Lu, Y. Li, R. Ganguly and R. Kinjo, *Angew. Chem., Int. Ed.*, 2017, **56**, 9829.

19 W. Lu, Y. Li, R. Ganguly and R. Kinjo, *J. Am. Chem. Soc.*, 2017, **139**, 5047.
20 W. Lu, Y. Li, R. Ganguly and R. Kinjo, *J. Am. Chem. Soc.*, 2018, **140**, 1255.
21 P. Bissinger, H. Braunschweig, A. Damme, T. Kupfer and A. Vargas, *Angew. Chem., Int. Ed.*, 2012, **51**, 9931.
22 P. Bissinger, H. Braunschweig, M. A. Celik, C. Claes, R. D. Dewhurst, S. Endres, H. Kelch, T. Kramer, I. Krummenacher and C. Schneider, *Chem. Commun.*, 2015, **51**, 15917.
23 H. Braunschweig, P. Bissinger, A. Damme, T. Kupfer, I. Krummenacher and A. Vargas, *Angew. Chem., Int. Ed.*, 2014, **53**, 5689.
24 S. R. Wang, M. Arrowsmith, H. Braunschweig, R. D. Dewhurst, V. Paprocki and L. Winner, *Chem. Commun.*, 2017, **53**, 11945.
25 H. Hommer, H. Nöth, J. Knizek, W. Ponikwar and H. Schwenk-Kircher, *Eur. J. Inorg. Chem.*, 1998, 1519.
26 A. Moezzi, M. M. Olmstead, R. A. Bartlett and P. P. Power, *Organometallics*, 1992, **11**, 2383.
27 H. Braunschweig, A. Damme, J. O. C. Jiménez-Halla, T. Kupfer and K. Radacki, *Angew. Chem., Int. Ed.*, 2012, **51**, 6267.
28 P. J. Domaille, J. D. Druliner, L. W. Gosser, J. M. Read Jr, E. R. Schmelzer and W. R. Stevens, *J. Org. Chem.*, 1985, **50**, 189.
29 M. Arrowsmith, J. Böhnke, H. Braunschweig, A. Deißenberger, R. D. Dewhurst, W. C. Ewing, C. Hörl, J. Mies and J. H. Müssig, *Chem. Commun.*, 2017, **53**, 8265.
30 H. Nöth and H. Vahrenkamp, *Chem. Ber.*, 1967, **100**, 3353.
31 L. Englert, A. Stoy, M. Arrowsmith, J. H. Müssig, M. Thaler, A. Deißenberger, A. Häfner, J. Böhnke, F. Hupp, J. Seufert, J. Mies, A. Damme, T. Dellermann, K. Hammond, T. Kupfer, K. Radacki, T. Thiess and H. Braunschweig, *Chem.–Eur. J.*, 2019, **25**, 8612.
32 N. Arnold, H. Braunschweig, A. Damme, R. D. Dewhurst, L. Pentecost, K. Radacki, S. Stellwag-Konertz, T. Thiess, A. Trumpp and A. Vargas, *Chem. Commun.*, 2016, **52**, 4898.
33 W. Clegg, M. R. J. Elsegood, F. J. Lawlor, N. C. Norman, N. L. Pickett, E. G. Robins, A. J. Scott, P. Nguyen, N. J. Taylor and T. B. Marder, *Inorg. Chem.*, 1998, **37**, 5289.
34 R. Schaeffer, Q. Johnson and J. Kane, *J. Am. Chem. Soc.*, 1970, **92**, 7614.
35 M. Arrowsmith, H. Braunschweig and T. E. Stennett, *Angew. Chem., Int. Ed.*, 2017, **56**, 96.
36 S. R. Wang, M. Arrowsmith, H. Braunschweig, R. D. Dewhurst, V. Paprocki and L. Winner, *Chem. Commun.*, 2017, **53**, 11945.
37 J. Ohshita, H. Ohsaki and M. Ishikawa, *Organometallics*, 1991, **10**, 2695.
38 M. A. Kropp and G. B. Schuster, *J. Am. Chem. Soc.*, 1989, **111**, 2316.
39 C. Fan, L. G. Mercier, W. E. Piers, H. M. Tuononen and M. Parvez, *J. Am. Chem. Soc.*, 2010, **132**, 9604.
40 J. H. Müssig, M. Thaler, R. D. Dewhurst, V. Paprocki, J. Seufert, J. D. Mattock, A. Vargas and H. Braunschweig, *Angew. Chem., Int. Ed.*, 2019, **58**, 4405.
41 H. Braunschweig, T. Brückner, A. Deißenberger, R. D. Dewhurst, A. Gackstatter, A. Gärtner, A. Hofmann, T. Kupfer, D. Prieschl, T. Thiess and S. R. Wang, *Chem.–Eur. J.*, 2017, **23**, 9491.
42 P. Bissinger, H. Braunschweig, A. Damme, R. D. Dewhurst, T. Kupfer, K. Radacki and K. Wagner, *J. Am. Chem. Soc.*, 2011, **133**, 19044.
43 N. Tsukahara, H. Asakawa, K.-H. Lee, Z. Lin and M. Yamashita, *J. Am. Chem. Soc.*, 2017, **139**, 2593.
44 Y. Shoji, T. Matsuo, D. Hashizume, H. Fueno, K. Tanaka and K. Tamao, *J. Am. Chem. Soc.*, 2010, **132**, 8258.